Am J Cancer Res 2016;6(10):2263-2276
www.ajcr.us /ISSN:2156-6976/ajcr0039717

Original Article

Hydroxyl-HIF2-alpha is potential therapeutic target for renal cell carcinomas

Takahiro Isono[1], Tokuhiro Chano[2], Tetsuya Yoshida[3], Susumu Kageyama[3], Akihiro Kawauchi[3], Masafumi Suzaki[1], Takeshi Yuasa[4]

[1]Central Research Laboratory, Departments of [2]Clinical Laboratory Medicine, [3]Urology, Shiga University of Medical Science, Otsu, Shiga 520-2192, Japan; [4]Department of Urology, Cancer Institute Hospital, Japanese Foundation for Cancer Research, Tokyo 135-8550, Japan

Received September 8, 2016; Accepted September 28, 2016; Epub October 1, 2016; Published October 15, 2016

Abstract: Dormant cancer cells are deprivation-resistant, and cause a number of problems for therapeutic approaches for cancers. Renal cell carcinomas (RCCs) include deprivation-resistant cells that are resistant to various treatments. In this study, the specific characteristics of deprivation-resistant cells were transcriptionally identified by next generation sequencing. The hypoxia-inducible factors (HIF) transcription factor network was significantly enhanced in deprivation-resistant RCCs compared to the sensitive RCCs. Deprivation-resistant RCCs, that had lost Von Hippel-Lindau tumor suppressor expression, expressed hydroxyl-HIF2-alpha in the nucleus, but not sensitive-RCCs. Hydroxyl-HIF-alpha was also expressed in nuclei of RCC tissue samples. Knockdown for HIF2-alpha, but not HIF1-alpha, induced cell death related to a reduction in HIF-related gene expression in deprivation-resistant RCC cells. Chetomin, a nuclear HIF-inhibitor, induced marked level of cytotoxicity in deprivation-resistant cells, similar to the knockdown of HIF2-alpha. Therefore, hydroxyl-HIF2-alpha might be a potential therapeutic target for RCCs.

Keywords: Hypoxia-inducible factors (HIF), hydroxyl-HIF-alpha, HIF2-alpha, renal cell carcinoma (RCC), chetomin, deprivation, Von Hippel-Lindau (VHL), global transcriptome, next generation sequencer (NGS), *POU5F1*

Introduction

Renal cell carcinoma (RCC) is the most common renal malignancy and is currently increasing in incidence [1]. In 2012, there were approximately 338,000 new cases and 144,000 deaths from RCC worldwide [2]. The increased use of abdominal imaging has led to the increased detection of the incidental renal masses, and consequently, the numbers of patients with localized RCC are increasing. However, more than 30% of newly diagnosed cases are to be regionally-advanced or at metastatic stages [1]. Radical nephrectomy remains the standard and only curative treatment for patients with localized RCC. However, up to half of the nephrectomized patients that appear cured eventually develop distant metastases. Therefore, effective anticancer drugs for metastatic RCC have been investigated, and several new molecular targeting drugs were developed [3]. Currently, two major subgroups of molecular targeting agents are used: tyrosine kinase inhibitors, including sorafenib, sunitinib, pazopanib and axitinib [4-8]; and specific inhibitors of the mammalian target of rapamycin (mTOR) kinase, temsirolimus and everolimus [9, 10]. The common mechanism of these agents is based on nutrient-deprivation of the tumor to inhibit tumor angiogenesis, rather than direct cytotoxicity. Glucose is one of the essential nutrients for cancer growth and is the major nutrient denied to cells following the inhibition of angiogenesis.

In previous studies, we searched for biomarkers and therapeutic targets of RCC by using two types of RCC cell lines [11, 12]. One type of cancer cells, which we termed "starvation-sensitive", produced *N*-linked (ß-*N*-acetylglucosamine)$_2$ [*N*-GlcNAc$_2$]-modified glycoproteins under glucose deprivation [13]. These glycoproteins promoted an unfolded protein response in the endoplasmic reticulum and the cells were in-

duced to G2/M cell cycle arrest causing a mitotic "catastrophe" [14], and death of the starvation-sensitive RCC cells [11]. The other type of cells, termed "starvation-resistant", did not show *N*-GlcNAc$_2$-modified protein accumulation or cell death; this behavior was quite similar to dormant-state cells under glucose deprivation [11]. Moreover, we demonstrated that starvation-resistant cells in RCCs possessed higher mitochondrial oxidative phosphorylation activity than starvation-sensitive cells [12]. In starvation-resistant cells, increased mitochondrial performance was supported by stored carbon sources, lipids and carbohydrates. Starvation-resistant cells also had lower mitochondrial reactive oxygen species (ROS) and higher superoxide dismutase (SOD) 2 expression.

This study analyzed the global transcriptional differences between deprivation- resistant RCC and deprivation-sensitive RCCs using a next generation sequencer to search for new biomarkers and therapeutic targets for RCCs. The analysis demonstrated that HIF2-alpha might be a potential therapeutic target for RCCs.

Materials and methods

Cell lines and cell culture conditions

We used seven RCC cell lines in this study: SW839, VMRC-RCW, KMRC-1, NC65, ACHN, Caki1 and Caki2. These cell lines were purchased from either the American Type Culture Collection, Riken Cell Bank, Cell Resource Center for Biomedical Research in Tohoku University or the Japanese Collection of Research Bioresources. All the cell lines were maintained in RPMI 1640 (Nacalai Tesque, Kyoto, Japan), which contained 25 mM glucose, supplemented with 10% fetal calf serum, penicillin (100 U/ml) and streptomycin (100 μg/ml) at 37°C in a humidified 5% CO_2 atmosphere. In the experimental culture, cells were seeded in high-glucose medium and then treated with or without the transfection of small interference RNA (siRNA) on day 1. The culture medium was then replaced with fresh high-glucose medium (25 mM glucose) or with glucose deprivation medium, which was depleted of glucose and sodium pyruvate (0 mM glucose, Nacalai Tesque) on day 2. On day 3 and 4, cells were used for some experiments. Treatments with chetomin (200 nM) were carried out when the medium was replaced on day 2.

RNA preparation

Total RNA from respective triplicate samples of SW839 and NC65 cells, grown in 25 mM of glucose, was extracted using acid guanidinium thiocyanate-phenol-chloroform [15]. The total RNA was quantified with a Bioanalyzer (Agilent, Santa Clara, CA) following the manufacturer's instructions. RIN (RNA Integrity Number) and A260/A280 ratio of the prepared total RNA were over 9.6, and over 1.5, respectively.

Illumina genome analyzer sequencing

The library of template molecules for high throughput DNA sequencing was converted from the total RNA using TruSeq RNA Sample Prep Kit v2 (Illumina, San Diego, CA) following the manufacturer's protocol. The library was quantified with a Bioanalyzer (Agilent) following the manufacturer's instructions. The library (4 pM) was subjected to cluster generation on a Single Read Flow Cell v4 (TruSeq SR Cluster Kit v2-cBot-GA) with a cBot instrument (Illumina). Sequencing was performed on a Genome Analyzer GAIIx for 37 cycles using TruSeq SBS Kit v5-GA regents (Illumina).

Data analysis

Image analysis and base calling were performed using Real Time Analysis version 1.13 (Illumina). Reads were aligned using ELAND v2 of CASAVA Software 1.8.2 with the sequence data sets of human genome build 19 (hg19), downloaded from the University of California, Santa Cruz genome browser (http://genome.ucsc.edu/). Transcript coverage for every gene locus was calculated from the total number passing filter reads that mapped to exons by ELAND-RNA. These analyses were performed using default parameters. The data were viewed using Genome Studio Software (Illumina). The advanced analysis for detecting significant pathways was performed using Avadis NGS software (version1.4, Strand Scientific Intelligence Inc., San Francisco, CA), as previously reported [14, 16]. The filterings were performed using default parameters. The genes with significantly different expressions were identified by the fold change method (fold change > 2), statistically analyzed by Benjamin-Hochberg's FDR ($P < 0.05$), and categorized into particular pathway categories by Find Significant Pathway analysis ($P < 0.05$). All new data has been deposited in the DDBJ under

Table 1. Oligonucleotides used for qRT-PCR

Gene symbol	Forward (5' to 3')	Reverse (5' to 3')
ABCB1	GATGCTGGTGTTTGGAGAAATGAC	TCCACTGTAATAATAGGCATACCTG
CA9	AATCAGAAGAAGAGGGCTCCCTG	TCGCCTCCATAGCGCCAATGAC
CP	AACTTAACAGCACCTGGAAGTGAC	ACCTCTGCCCAAATGACAGGAC
EGLN3	TTACGCAACCAGATATGCTATGAC	TCTTCAGTGAGGGCAGATTCAG
HIF1	CATGTGACCATGAGGAAATGAGAG	CATGTTAGGGTACACTTCATTCTG
HIF2	CGACCATGAGGAGATTCGTGAG	CGTGCAGTGCAAGACCTTCCAG
HK1	CCAAAATAGATGAGGCCATCCTG	AGCTACGATGTTGGCATCATAGTC
HMOX1	GAGCGTCCGCAACCCGACAG	TACAGGGAGGCCATCACCAGC
NDRG1	AGTTTGATGTCCAGGAGCAGGAC	AGTTGAAGAGGGGGTTGTAGCAG
NK5E	CAACATGGGCAACCTGATTTGTG	CCAGGTTCTCCCAGGTAATTGTG
PLIN2	TGCCCATCATCCAGAAGCTAGAG	CTTTGGCATTGGCAACAATCTGAG
POU5F1	CAAAACCCGGAGGAGTCCCAG	CCTCAAAGCGGCAGATGGTCG
SLC2A1	AGCCCAGCAGCAAGAAGCTGAC	GCTCTCCCCATAGCGGTGGAC
GAPDH	GGGAGCCAAAAGGGTCATCATC	TGGCATGGACTGTGGTCATGAG
VHL	F1: GGTGGTCTGGATCGCGGAGG	R1: CATCAAAAGCTGAGATGAAACAGTG
	F2:GCGTCGTGCTGCCCGTATGG	R2: CTGCATCTCTGAAGAGCCAAAGG

accession number DRA005074, PRJDB5127, and SAMD00058068-73.

Antibodies

The anti-HIF-1 α (#14179) and Hydroxy-HIF-1 α (Pro564) (#3434) rabbit monoclonal antibodies were purchased from Cell Signaling Technology (Beverly, MA). The anti-HIF-2 α (NB-100-122) rabbit polyclonal antibodies were purchased from Novus Biologicals (Littleton, CO). The anti-Lamin B (C-20: sc-6216) goat polyclonal antibodies were purchased from Santa Cruz Biotechnology (Santa Cruz, CA). The anti-α-tubulin (#T9026, DM1A) and anti-ß-tubulin (#T4026, TUB2.1) monoclonal antibodies were purchased from Sigma-Aldrich (St. Louis, MO).

Immunoblotting

Cells were lysed in Laemmli-SDS buffer, subjected to SDS-polyacrylamide gel electrophoresis, and electro-transferred to membrane filters (Immuno-Blot PVDF membranes, Bio-Rad Laboratories, Richmond, CA). The filters were incubated overnight with a primary antibody in TBS-T containing 2% bovine serum albumin and incubated for 1 hour in horseradish peroxidase-conjugated anti-mouse, anti-rabbit (Cell Signaling Technology), or anti-goat secondary antibodies (Santa Cruz Biotechnology) diluted 1: 5,000 in TBS-T containing 2% bovine serum albumin. Immunoreactivity was detected using the Luminata Classico Western HRP substrate (Millipore Corporation) with LAS4000 (Fujifilm, Tokyo, Japan) and quantified with MultiGauge software (Fujifilm), using an anti-α-tubulin antibody as the internal control.

Immunofluorescence staining

Cells were cultured in 35 mm glass bottomed dishes (Matsunami Glass, Osaka, Japan). For the immunofluorescence staining, the medium was removed and the cells were fixed with 4% paraformaldehyde for 5 minutes and then permeabilized with 0.1% Triton X-100 for 5 minutes. The cells were washed three times with phosphate buffer saline before being incubated with a primary antibody overnight. Cells were then incubated with a secondary fluorescence-labeled anti-rabbit IgG (Alexa Fluor 488, Life Technologies, Carlsbad, CA) for 1 hour. Nuclei were stained by DAPI (NucBlue Fixed Cell Stain ReadyProbes reagent, Life Technologies). Samples were observed using a Nikon C1si confocal fluorescent microscope (Nikon, Tokyo, Japan). RCC specimens obtained by radical/partial nephrectomy in the Department of Urology of Shiga University of Medical Science Hospital were fixed in 10% buffered formalin for approximately 48 hours, and then embedded in paraffin. Four μm thick sections were made, and the slides were autoclaved (120°C, 1 min) for antigen-retrieval, after deparaffinization and rehydration. RCC tissue specimens were treated and observed as for immunocytofluorescence.

Cell viability

Cells (4×10^4) were plated onto 24-well culture plates and cultured at 37°C. For the cell viability assay, cells were stained with 0.1% trypan blue and the proportions of living and dead cells were determined.

Table 2. Up (A) and down (B)-regulated pathways in SW839 vs NC65 under 25 mM glucose conditions by find significant pathway analysis

A			
Pathway	Matched with Technology*	Matched with EntityList†	*p* value‡
Metabolism of lipids and lipoproteins	136	46	9.90E-06
Syndecan-4-mediated signaling events	164	52	1.87E-05
Proteogylcan syndecan-mediated signaling events	35	16	8.02E-05
L1CAM interactions	26	12	1.96E-04
Superpathway of cholesterol biosynthesis	24	12	2.21E-04
HIF-1-alpha transcription factor network	57	24	2.40E-04
Syndecan-2-mediated signaling events	61	22	3.06E-04
Shortest Connect	36	15	3.74E-04
Ephrin B reverse signaling	13	8	4.19E-04
Beta3 integrin cell surface interactions	19	10	4.41E-04
B			
Pathway	Matched with Technology*	Matched with EntityList†	*p* value‡
Expand Interactions	235	69	6.84E-05
Dermatan sulfate biosynthesis	12	8	3.26E-04
Chondroitin sulfate biosynthesis	15	9	4.20E-04
tRNA Aminoacylation	18	9	0.002387
Resolution of AP sites via the single-nucleotide replacement pathway	11	7	0.004386
Organic cation transport	5	4	0.004945
p53 pathway	156	44	0.005144
Class I PI3K signaling events mediated by Akt	191	52	0.005614
p63 transcription factor network	89	28	0.006014
DNA Repair	53	19	0.007936

*: The gene number on the pathway, according to databases. †: The number of genes that were statically up and down-regulated in SW839 cells. ‡: In Find signification Pathway analysis (Avadis NGS), Fisher's exact test was applied for the significance of EntityList among up and down-regulated genes.

Quantitative reverse-transcription-polymerase chain reaction (qRT-PCR)

Total RNAs were obtained from RCC cells by acid guanidinium thiocyanate-phenol-chloroform. Quantitative RT-PCR was performed using the LightCycler 480 SYBG Master I Mix and LightCycler 480 System II (Roche Diagnostics, Mannheim, Germany). Gene expression was normalized against the *GAPDH* gene. Primer sequences are listed in **Table 1**. All quantification analyses were performed in triplicate.

siRNA

siRNAs targeting human *HIF1A* (s6541), *HIF2A/EPAS1* (s4698 and s4699), and *POU5F1* (s10873) RNA duplexes were purchased from Life Technologies. Scrambled control RNA duplexes (Silencer Select Negative Control #1 siRNA, 4390844) were also purchased from Life Technologies. Cells were transfected with RNA duplexes using Lipofectamine RNAiMAX reagents (Life Technologies) following the manufacturer's protocol.

Nuclear extraction

Nuclear and cytoplasmic fractions were extracted from cells cultured in 100-mm dishes by NE-PER Nuclear and Cytoplasmic Extraction Reagents (Thermo Fisher Scientific, Rockford, IL).

Statistics

The data are reported as means ± standard error. The values were derived from at least triplicate experiments. Student's *t*-test (two-tail)

Table 3. List of genes among "HIF-1-alpha transcription factor network" that were significantly up-regulated two-fold in SW839 vs NC65 under 25 mM glucose conditions

Gene symbol	t-test (*p* value)	Fold change
ABCB1	3.78E-07	758.62427
BHLHE41	0.001354086	3.9571972
BNIP3	0.001919574	2.8725636
CA9	1.40E-04	10.634261
CP	0.001568328	600.75336
CREB1	0.012886733	2.4445403
CXCL12	0.00114748	35.513268
DNAJC3	0.001352736	2.3862236
EDN1	0.007599767	9.105965
EGLN1	0.003206002	2.0212307
EGLN3	2.40E-04	6.829358
F2R	5.09E-05	4384.394
GCK	0.0048169	18.206501
HK1	5.33E-05	10.342828
HMOX1	1.26E-04	6.3594265
ID2	4.85E-04	3.8716807
ITGB2	0.001698479	3.999043
NDRG1	2.93E-04	4.257388
NT5E	2.17E-04	23.792044
PFKFB3	8.18E-05	10.234147
PLIN2	1.49E-04	11.291362
SERPINE1	3.12E-06	42.976315
SLC2A1	6.60E-04	3.554851
SRSF11	0.01978133	2.3452723

was used to compare differences between groups.

Results

The HIF transcription factor network is significantly enhanced in deprivation-resistant RCCs as assessed by global transcriptomics and qRT-PCR

Global transcriptomics was used to profile a deprivation-resistant RCC, SW839, in respect to a deprivation-sensitive RCC, NC65. We analyzed genes that were differentially expressed between SW839 and NC65 cells using the 'Find Significant Pathway' analysis software package (Avadis NGS software version 1.4, **Table 2**). **Table 2** shows the top 10 most significantly up- and down-regulated pathways. In the deprivation-resistant SW839 cells, "DNA repair" and "nucleotide replacement pathways" were down-regulated compared with NC65 cells. Three pathways; "metabolism of lipids and lipoproteins", "superpathway of cholesterol biosynthesis", and "HIF-1-alpha transcription factor network", were up-regulated. According to the Pathway Interaction Database, the "superpathway of cholesterol biosynthesis" shares similar genes to the "metabolism of lipids and lipoproteins" pathway, indicating these two pathways may be controlled by a common mechanism. In a previous study, we suggested that deprivation-resistant RCCs might be clear cell RCCs, which lacked the Von Hippel-Lindau *(VHL)* gene and have non-functioning HIF transcription [12]. In this study, we focused on the HIF transcription factor network pathway.

In SW839 cells, 24 genes belonging to the "HIF-1-alpha transcription factor network pathway" were listed as up-regulated genes (two fold increments) compared with NC65 cells (**Table 3**). We evaluated the expression of half of these genes in three deprivation-resistant RCCs and four deprivation-sensitive RCCs using qRT-PCR analysis (**Table 4**). Three of the 12 genes, *NDRG1*, *PLIN2*, and *SLC2A1*, were significantly up-regulated in deprivation-resistant RCCs compared with deprivation-sensitive RCCs. For the expression of *ABCB1* and *HMOX1*, three deprivation-resistant RCCs were ranked in the top three of seven RCCs. The other genes without *HK1* tended to show an increase in the deprivation-resistant RCCs. *SLC2A1*, *EGLN3*, and *SERPIN1* belong to both "HIF-1-alpha and 2-alpha transcription factor network pathways". The data showed that the "HIF transcription factor network" was enhanced in deprivation-resistant RCCs compared with deprivation-sensitive RCCs.

Deprivation-resistant RCCs express hydroxyl-HIF in nuclei, and lose VHL expression

Clear cell RCCs often carry genetic anomalies of the VHL tumor suppresser, inhibiting HIF1- and 2-alpha activities by ubiquitination [17]. However, the status of VHL expression is controversial in several cell lines [12]. Therefore, we confirmed the *VHL* gene status of all the seven RCCs using direct sequencing (**Table 5**). All three deprivation-resistant RCCs (SW839, VMRC-RCW and KMRC-1) showed genetic anomalies of *VHL*, and almost all deprivation-sensitive RCCs showed the wild-type *VHL* form,

Table 4. Quantitative RT-PCR data of renal cell carcinomas for genes belonging to the "HIF transcription factor network"

Gene symbol	Resistant SW839	VMRC-RCW	KMRC-1	Sensitive NC65	ACHN	Caki1	Caki2S	Resistant vs Sensitive
ABCB1	1.00	*11.44*	*1.92*	**0.00**	**0.30**	**0.56**	0.58	0.191
CA9	1.00	*5.28*	**0.01**	**0.49**	0.02	**0.00**	**0.00**	0.208
CP	1.00	*7.27*	*44.90*	**0.00**	**0.00**	**0.19**	1.14	0.190
EGLN3	1.00	1.18	**0.12**	0.36	**0.00**	**0.01**	*1.24*	0.446
HK1	1.00	**0.75**	*1.88*	**0.11**	0.95	*1.70*	1.05	0.612
HMOX1	1.00	*1.27*	*3.68*	**0.07**	**0.20**	0.25	**0.22**	0.054
NDRG1	1.00	*1.85*	0.92	0.35	**0.06**	**0.13**	**0.17**	0.009
NT5E	1.00	*1.65*	*3.35*	**0.07**	*1.41*	*2.63*	**0.57**	0.391
PFKFB3	1.00	**0.62**	0.39	**0.03**	**0.09**	**0.33**	**0.47**	0.070
PLIN2	1.00	*1.44*	**0.53**	**0.05**	**0.13**	0.19	**0.06**	0.004
SERPINE1	1.00	0.42	*30.16*	**0.03**	**0.22**	*5.74*	**0.02**	0.331
SLC2A1	1.00	**0.48**	*1.63*	**0.12**	**0.17**	**0.08**	0.31	0.028
POU5F1	1.00	*1.73*	*2.54*	**0.21**	**0.13**	**0.19**	0.64	0.020
HIF1	1.00	**0.48**	**0.00**	**0.28**	*4.59*	*3.14*	1.02	0.199
HIF2	1.00	*2.45*	*3.00*	**0.58**	1.44	*2.64*	**0.03**	0.295

Gene expressions were normalized to *GAPDH*, and base-lined with those of SW839. The values represent data from triplicate experiments. The Student's *t*-test (two-tailed) was used to compare statistical differences between both groups. Italics and bold texts indicate the up- and down-regulation of expression vs SW839 ($P < 0.05$), respectively. Red and green texts indicate the top three and median, respectively. Oranges indicate statistical differences between starvation-resistant and starvation-sensitive RCCs ($P < 0.05$).

Table 5. VHL status in renal cell carcinomas

Cell lines	VHL status		
		Sequencing	
SW839	Mutant	Not amplified	Frame shift*
VMRC-RCW	Mutant	2 bp deletion	Frame shift
KMRC-1	Mutant	3 bp deletion	1aa (Phe) deletion
NC65	Wild	No mutation	
Caki1	Wild	No mutation	
Caki2	Mutant	Point mutation	Stop codon
ACHN	Wild	No mutation	

*: Shinojima T, Oya M, Takayanagi A, Mizuno R, Shimizu N, Murai M. Renal cancer cells lacking hypoxia inducible factor (HIF)-1a expression maintain vascular endothelial growth factor expression through HIF-2a. Carcinogenesis 2007; 28: 529-536.

with one exception (Caki2). These results are consistent with the data that the "HIF transcription factor network" was enhanced in deprivation-resistant RCCs, compared with the deprivation-sensitive RCCs.

We investigated the HIF1- and 2-alpha expression in seven RCCs using immunoblotting (**Figure 1A**). In the four RCCs with *VHL* gene anomalies, SW839 and VMRC-RCW expressed both HIF1- and 2-alpha. KMRC-1 or Caki2 expressed either HIF 2-alpha or HIF 1-alpha. Because there were no significant differences between resistant- and sensitive-RCCs for the transcription of HIF1- and 2-alpha (**Table 4**), HIF2-alpha proteins might be the difference between both types of RCCs and explain the enhanced characteristic of the "HIF transcription factor network" in deprivation-resistant RCCs. Indeed, *POU5F1* (Oct3/4), which is restricted in "HIF-2-alpha transcription factor network pathway", was significantly up-regulated only in deprivation-resistant RCCs (**Table 4**). This is consistent with a report that the expression of *PLIN2* was associated with HIF2-alpha but not HIF1-alpha [18].

We also investigated whether hydroxy-HIF1- and 2-alpha proteins sub-localized with the transcription factors in cell nuclei (**Figure 1B**). In four RCCs containing VHL anomalies, hydroxy-HIF1- and 2-alpha proteins mainly existed in the nuclear extract. These results were confirmed by immunofluorescent analysis using anti-hydroxy-HIF1-alpha antibodies (**Figure 2A**), which cross-react with hydroxy-HIF2-alpha: thus indicating the nuclear presence of hydroxylated forms of both HIF1 and 2 (**Figure**

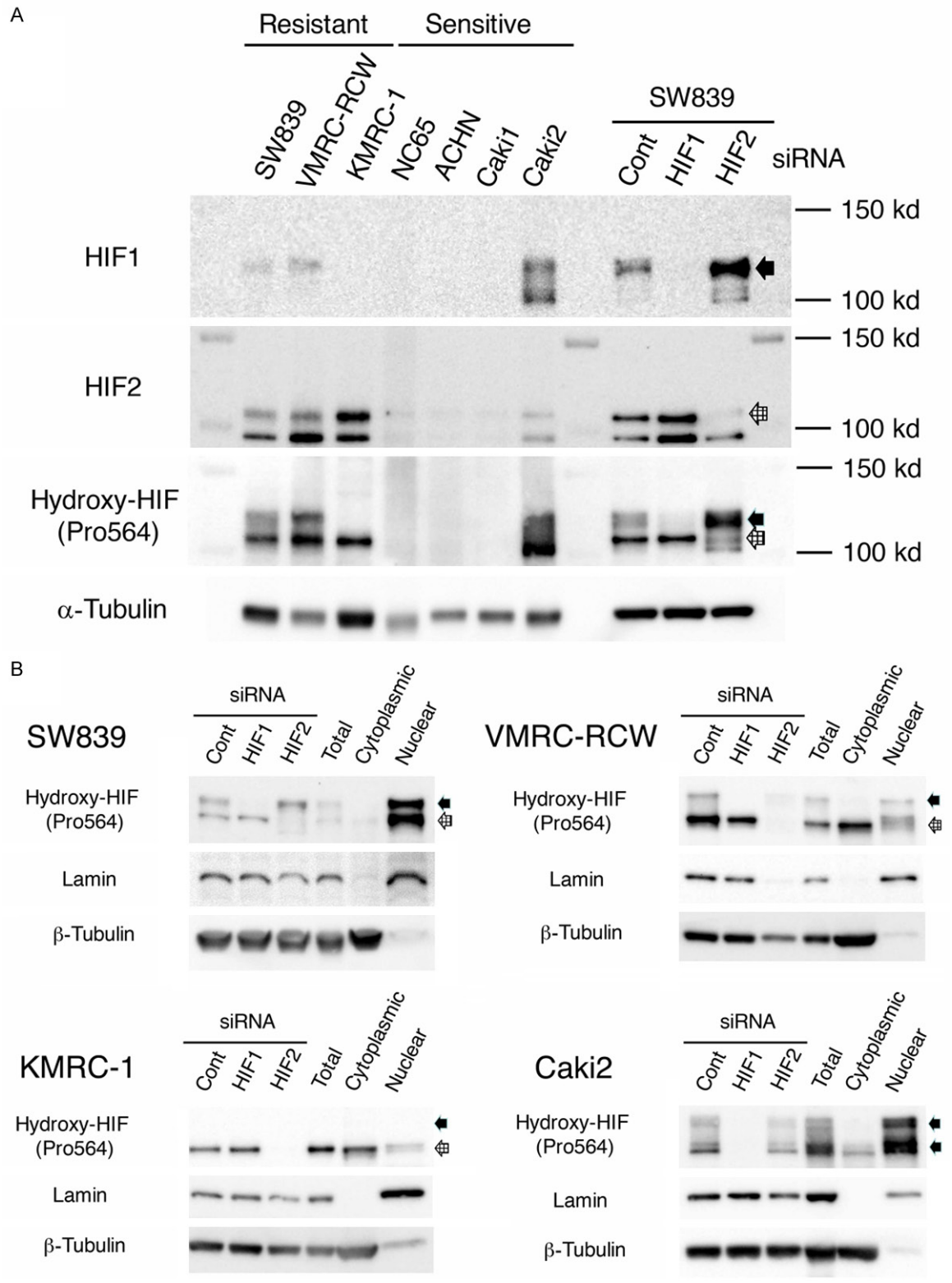

Figure 1. Immunoblot data of HIF1- and HIF2-alpha in RCC cell lines: A. Immunoblots for HIF1- and HIF2-alpha, hydroxyl-HIF (Pro564), and α-tubulin for whole cell extracts of seven RCCs. B. Immunoblots for hydroxyl-HIF, Lamin B and ß-tubulin for cytoplasmic and nuclear extracts of four HIF-expressing cell lines, which lacked the normal *VHL* gene. Note that the four RCCs lacked the normal *VHL* gene, SW839 and VMRC-RCW cells expressed both HIF1- and HIF2-alpha, KMRC-1 cells only expressed HIF 2-alpha, and Caki2 only expressed HIF 1-alpha. HIF1- and HIF2-alpha proteins were modified by hydroxylation and localized with transcription factors in cell nuclei. These results suggested that the difference between deprivation-resistant and deprivation-sensitive RCCs was caused by the presence of HIF2-alpha.

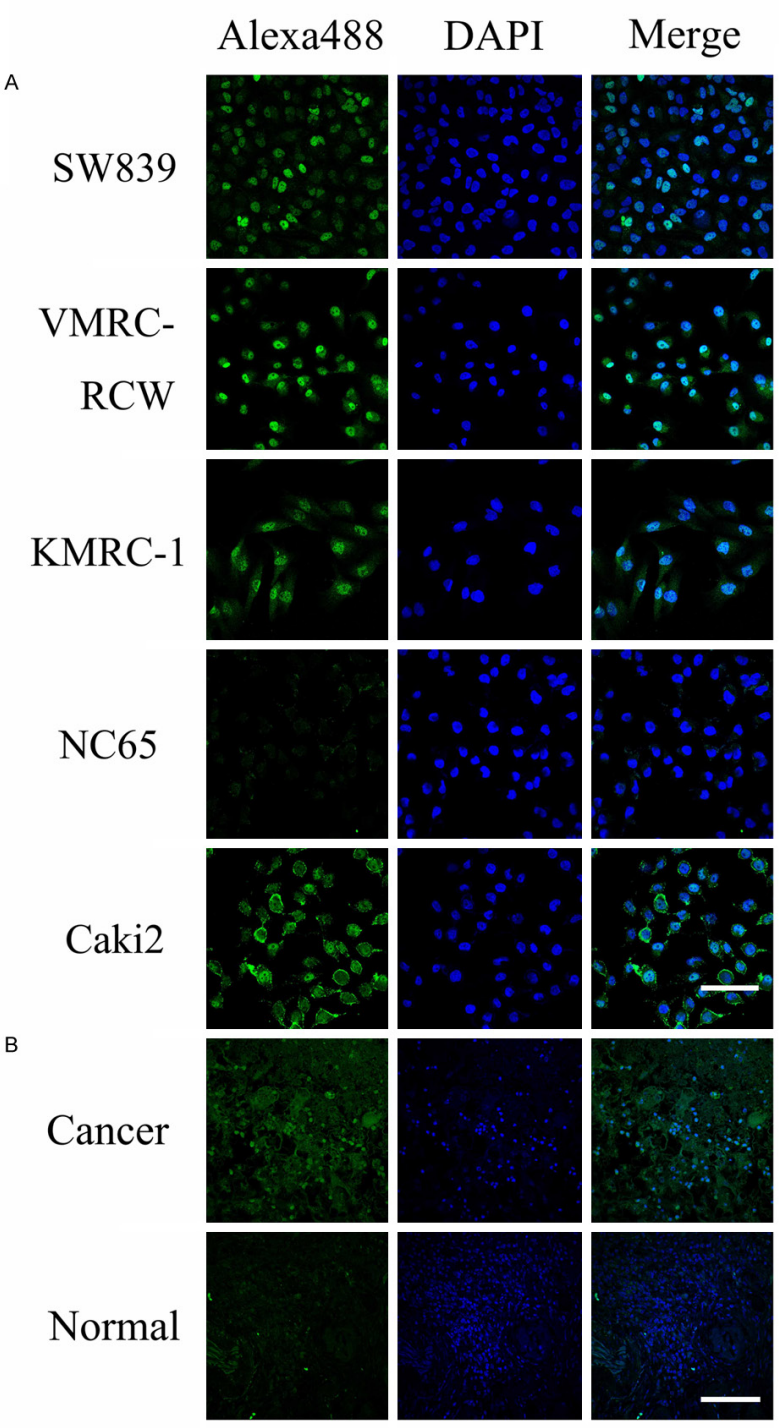

Figure 2. Immunofluorescence data of HIF1- and HIF2-alpha in RCCs. Photographs of Alexa 488: (marked with anti-hydroxy HIF antibodies, left), DAPI (central) and their merging (right) in four RCCs (SW839, VMRC-RCW, KMRC-1 and Caki2) and aNC65 containing *VHL* anomalies and normalcy, respectively, (A); and clinical RCC tissues (B). The scale bars correspond to 100 μm. Hydroxy-HIF1- and HIF2-alpha proteins mainly existed in the cellular nuclei of the four RCCs containing *VHL* anomalies. These results suggested that hydroxy-HIF2-alpha acts as a nuclear transcription factor in deprivation-resistant RCCs, and that hydroxy-HIF proteins are also localized in the RCC nuclei of clinical human samples.

1A). These results suggested that both hydroxylated forms are present in cell nuclei of RCCs, where the ubiquitinated degradation cannot be induced by VHL anomalies even under normal oxidation. Hydroxy-HIF signals were also localized in cancer cell nuclei by the immunofluorescence analysis of clinical RCC samples (**Figure 2B**).

Knockdown of HIF2-alpha but not HIF1-alpha induced cell death with HIF-related gene reduction in deprivation-resistant RCCs

To clarify the contribution of HIF2-alpha to deprivation-resistant RCCs, siRNA for HIF2-alpha (s4699) was introduced into all three deprivation-resistant RCCs, and caused cell death in cultures with 25 mM glucose, in contrast to HIF1-alpha- or control-siRNA (**Figure 3**). The cell death was similarly caused by another siRNA for HIF2-alpha (s4698). Similar results were observed in cultures without glucose (data not shown). Cell death was not induced by HIF1- or 2-alpha knockdown under 25 mM glucose conditions in NC65, which do not express HIF1- or HIF2-alpha, or in Caki2, which only express HIF1-alpha. Therefore, the survival of deprivation-resistant RCCs might depend on HIF2-alpha, although these cells survived without nutrients.

Moreover, the effect of HIF2 siRNA was evaluated by qRT-PCR for the expressions of six genes, up-regu-

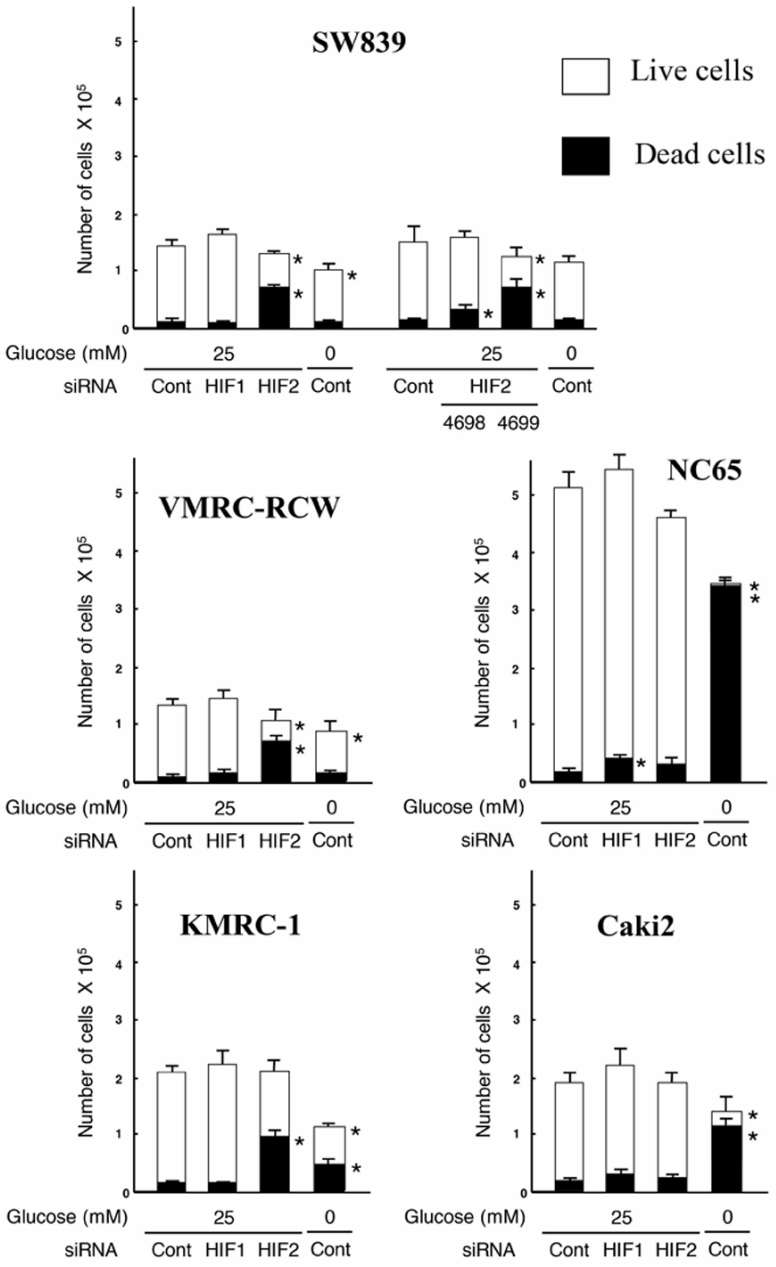

Figure 3. The cytotoxic effects of HIF1- or HIF2-alpha siRNA knockdown to RCCs. Starvation-resistant cell lines, SW839, VMRC-RCW, and KMRC-1, and starvation-sensitive cell lines, NC65 and Caki2, were seeded in 25 mM glucose medium, and then treated with specific siRNAs for HIF1-alpha (s6541), HIF2-alpha (s4699) or scrambled control siRNA on day 1. SW839 cells were also treated with another kind of specific siRNA for HIF2-alpha (s4698). The culture medium was then replaced on day 2 with 25 mM or 0 mM glucose medium, and cells were collected on day 3. The numbers of living and dead cells were counted using the trypan-blue exclusion assay. Error bars represent the standard errors from triplicate experiments. Asterisks (*) indicate statistically significant differences ($P < 0.05$) with respect to the numbers of living (upper) or dead cells (lower) under control conditions (25 mM glucose with control siRNA). Note that HIF2-alpha knockdown, but not HIF1-alpha knockdown, induced cell death in all three deprivation-resistant RCCs cultured with 25 mM glucose. HIF1- or HIF2-alpha knockdown did not induce cell death in two deprivation-sensitive RCCs cultured with 25 mM glucose, although deprivation-sensitive RCCs died in the absence of glucose. The survival of deprivation-resistant RCCs might depend on HIF2-alpha, although these cells were resistant to glucose deprivation.

lated specifically in deprivation-resistant RCCs, (**Table 6**). *PLIN2* and *POU5F1* corresponded most consistently to cell survival under the knockdown experiments in RCCs. *NDRG1*, *PLIN2*, and *POU5F1* were significantly down-regulated in all of three deprivation-resistant RCCs by knockdown of HIF2-alpha, but not HIF1-alpha. *ABCB1*, *HMOX*, and *SLC2A1* were not significantly down-regulated in all three RCCs. In KMRC-1 that only express HIF2-alpha, all six genes were significantly down-regulated by HIF2-alpha siRNA. SW839 and VMRC-RCW cells that express both HIF1- and 2-alpha might be mutually compensated by the up-regulation of HIF1-alpha under HIF2-alpha knockdown conditions. In Caki2 that only express HIF1-alpha, *NDRG1* were significantly down-regulated.

To determine whether the cell death of deprivation-resistant RCCs under HIF2-alpha knockdown was caused by its transcriptional function, we investigated the effect of chetomin, an inhibitor of the transcriptional function of HIF1 and HIF2 in cell nuclei [19]. Chetomin caused cell death in all deprivation-resistant RCCs, but not in two kind of deprivation-sensitive RCCs, quite similarly to the experimental data for the HIF2-alpha siRNA experiments (**Figure 4**). Chetomin inhibits the transcriptional functions of both HIF1 and HIF2, suggesting that cell death caused by HIF2-alpha knockdown did not correspond to the knockdown of HIF1-alpha, but rather to the

Table 6. The inhibitory effects of s HIF1- or HIF2-alpha siRNA on genes belonging to the "HIF transcription factor network" in RCCs

	HIF1	*HIF2*	*ABCB1*	*HMOX1*	*NDRG1*	*PLIN2*	*SLC2A1*	*POU5F1*
SW839								
siControl	1.00	1.00	1.00	1.00	1.00	1.00	1.00	1.00
siHIF1	**0.23**	*1.67*	1.11	*1.80*	1.04	*1.40*	0.87	0.99
siHIF2	*1.36*	**0.20**	1.12	0.98	**0.76**	**0.63**	**0.80**	**0.69**
VMRC-RCW								
siControl	1.00	1.00	1.00	1.00	1.00	1.00	1.00	1.00
siHIF1	**0.44**	1.07	1.14	1.17	0.96	*1.34*	1.21	*1.19*
siHIF2	*1.51*	**0.18**	**0.73**	0.89	**0.34**	**0.42**	0.95	**0.73**
KMRC-1								
siControl	n.d.	1.00	1.00	1.00	1.00	1.00	1.00	1.00
siHIF1	n.d.	1.10	1.06	*1.40*	1.08	*1.24*	1.06	0.90
siHIF2	n.d.	**0.15**	**0.65**	**0.36**	**0.17**	**0.61**	**0.34**	**0.33**
NC65								
siControl	1.00	1.00	n.d.	1.00	1.00	1.00	1.00	1.00
siHIF1	**0.07**	1.22	n.d.	*1.26*	1.08	1.02	0.98	1.47
siHIF2	1.26	**0.15**	n.d.	1.19	*1.38*	*1.38*	*1.56*	*2.02*
Caki2								
siControl	1.00	1.00	1.00	1.00	1.00	1.00	1.00	1.00
siHIF1	**0.20**	*1.59*	*1.36*	*1.55*	**0.59**	1.15	1.13	0.98
siHIF2	*1.29*	**0.14**	0.81	0.94	1.16	1.16	1.10	1.35

Gene expressions were normalized to *GAPDH*, and base-lined by those with control siRNA. The values were represent data from triplicate experiments. The Student's *t* -test (two-tailed) was used to compare statistical differences of each siRNA with control siRNA (siRNA). Italics and bold texts indicate the up- and down-regulation vs the expression with control siRNA ($P < 0.05$), respectively. "n.d." not detectable.

inhibitory knockdown of HIF2-alpha in deprivation-resistant RCCs.

Taken together, HIF2-alpha is likely to be involved in malignant transformation as a nuclear transcriptional factor by regulating the gene expressions of *PLIN2* and *POU5F1*, and to contribute to the survival of deprivation-resistant RCCs. Knockdown of *POU5F1* did not induce cell death in the deprivation-resistant RCCs, but partially reduced the cell growth (**Figure 5**).

Discussion

The present study demonstrated that hydroxy-HIF2-alpha was likely to contribute to the survival of deprivation-resistant RCCs by regulating the expressions of specific genes.

According to the global transcriptomic analysis used to profile a deprivation-resistant RCC, SW839, "DNA repair" and "nucleotide replacement pathways" were down-regulated compared to a deprivation-sensitive RCC, NC65. Previously, deprivation-resistant RCCs showed less mitochondrial ROS, indicating similarities with dormant state cells, where DNA damage is accompanied by ROS expression [12]. In addition, three important pathways "metabolism of lipids and lipoproteins", "superpathway of cholesterol biosynthesis", and "HIF transcription factor network", were up-regulated. These pathways are highly likely to correlate with the characteristics of clear cell RCCs [20]. Deprivation-resistant RCCs store more sources of carbon, lipids and carbohydrates, and can survive even under nutritive deprivation. Therefore, they have a similar capacity to malignant dormant cells [12]. In deprivation-resistant RCCs, the lipid store must be naturally supported by the up-regulation of the metabolism of lipids and lipoproteins pathway. To identify new biomarkers and therapeutic targets for RCCs, it was necessary to profile deprivation-resistant RCCs, which have similar characteristics to malignant dormant cells. The

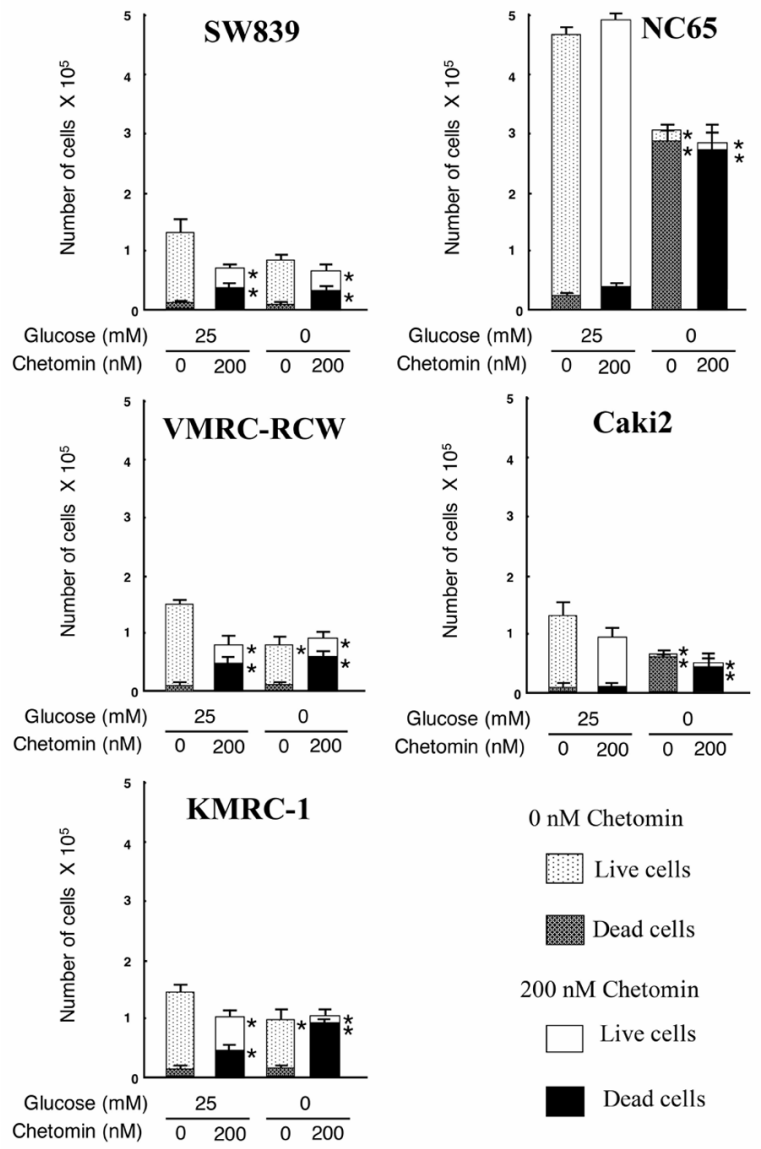

Figure 4. Chetomin, an HIF inhibitor, affects the cell death of RCCs. Starvation-resistant cells, SW839, VMRC-RCW and KMRC-1, and starvation-sensitive cell lines, NC65 and Caki2, were seeded in 25 mM glucose medium on day 1. The culture medium was then replaced on day 2 with 25 mM or 0 mM glucose medium with or without 200 nM chetomin, and cells were collected on day 3. The numbers of living and dead cells were counted using the trypan-blue exclusion assay. Error bars represent the standard errors from triplicate experiments. Asterisks (*) indicate statistically significant differences ($P < 0.05$) with respect to the numbers of living (upper) or dead cells (lower) under control conditions (25 mM glucose without chetomin). Note that chetomin induced cell death in three deprivation-resistant RCCs, but not in two deprivation-sensitive RCCs; similar to that for HIF2-alpha knockdown (**Figure 4**). This suggests that the cell death of deprivation-resistant RCCs caused by HIF2-alpha knockdown might be due to the inhibitory function of the HIF2-alpha transcription factor.

various analyses suggested that hydroxyl-HIF2-alpha might be a useful biomarker and possible therapeutic target for RCCs.

Our results also suggested that HIF inhibitors like chetomin are effective for HIF2-alpha abundant RCCs. However, chetomin had no function on a deprivation-sensitive RCC, Caki2, containing HIF1-alpha and lacking normal *VHL*. The single inhibition of HIF2-alpha may be insufficient to prevent the development of all VHL-defective malignancies, and therefore a combination of various inhibitors for both HIF and angiogenesis should be recommended for the treatment for RCC patients.

It was previously reported that HIF2-alpha-expressing RCCs were more malignant than HIF1-alpha-expressing RCCs [17], and that the knockdown of HIF2-alpha induced the cell death and/or reduced the cell growth for RCCs in both cell lines and mice xenograft models [17, 18, 21, 22]. We showed that the death of deprivation-resistant RCCs caused by HIF2-alpha knockdown might be explained by the regulation of *PLIN2* and *POU5F1* expression. Although a previous report showed that cancer cell viability was reduced by *PLIN2* knockdown [18], which is an important gene in the HIF transcription factor pathway, and corresponded consistently with cell survival under HIF knockdown experiments in RCCs, the knockdown of *POU5F1* (or for *PLIN2*; data not shown) did not induce cell death in deprivation-resistant RCCs, but partially reduced cell growth. This discrepancy might due to the similar characteristics of deprivation-resistant RCCs and malignant dormant cells, which often become resistant to various molecular targeting agents, based on

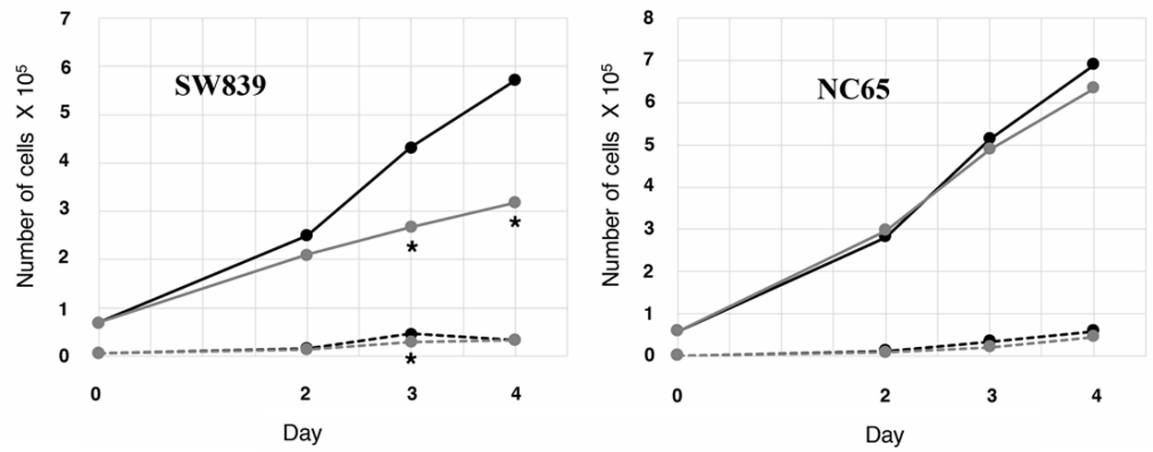

Figure 5. Knockdown of *POU5F1* partially affects cell death in RCCs. Starvation-resistant cell lines, SW839, and a starvation-sensitive cell line, NC65, were seeded in 25 mM glucose medium, and then treated with *POU5F1* siRNA or scrambled control siRNA after 24 h (day 0). Cells were collected on days 2-4. The numbers of living and dead cells were counted using the trypan-blue exclusion assay. The experiments were performed in triplicate. Solid and interrupted lines show live and dead cell numbers, respectively. Grey or black lines show cells treated with *POU5F1* siRNA or scrambled control siRNA, respectively. Asterisks (*) indicate statistically significant differences ($P < 0.05$) with respect to the cell numbers treated with siRNA control. Note that knockdown for *POU5F1* reduced cell growth in SW839 cells, but not in NC65 cells.

nutrient-deprivation via the inhibition of tumor angiogenesis [9, 10]. Alternatively, hydroxy-HIF2-alpha may control unknown genes, because deprivation-resistant RCCs did not show the upregulation of canonical genes such as the vascular endothelial growth factor A gene (*VEGFA*), belonging to "HIF-2-alpha transcription factor network". However, further studies will be needed to identify this mechanism.

An immunofluorescence assay indicated that anti-hydroxy-HIF signals weren't only localized in RCC cell lines, but also in human RCC tissues. Staining with anti-hydroxy-HIF1-alpha antibodies were also reported in breast cancer patient samples [23]. Hydroxy-HIF signals, which were preferably detected and were due mainly to HIF2-alpha in deprivation-resistant RCCs, might be a useful biomarker in the clinical setting of RCCs.

In conclusion, hydroxyl-HIF2-alpha might be a useful biomarker in the clinical setting of RCCs and a potential therapeutic target for the treatment of RCC patients. Further stu dies are needed to understand the full contribution of hydroxy-HIF2-alpha to the survival of deprivation-resistant RCCs.

Acknowledgements

We thank Mr. Takefumi Yamamoto, Ms. Hiroko Kita and Ms. Kimiko Kimura (Shiga University of Medical Science) for assistance with immunofluorescence observations, preparation of immunofluorescence samples, and qPCR analysis, respectively. The work was supported by the Smoking Research Foundation (T. Y.); JSPS KAKENHI Grant Numbers 15K06854 (T. I.), 25293130 (T. C.), 26460648 (T. C.), 15K10584 (S. K.), 16K11035, and 25462504 (T. Y.).

Disclosure of conflict of interest

None.

Address correspondence to: Takahiro Isono, Central Research Laboratory, Shiga University of Medical Science, Otsu, Shiga 520-2192, Japan. Tel: +81-77-548-2308; Fax: +81-77-548-2049; E-mail: isono@belle.shiga-med.ac.jp

References

[1] Siegel RL, Miller KD, Jemal A. Cancer statistics, 2015. CA Cancer J Clin 2015; 65: 5-29.
[2] Ferlay J, Soerjomataram I, Dikshit R, Eser S, Mathers C, Rebelo M, Parkin DM, Forman D,

Bray F. Cancer incidence and mortality worldwide: sources, methods and major patterns in GLOBOCAN 2012. Int J Cancer 2015; 136: E359-86.

[3] Ljungberg B, Bensalah K, Canfield S, Dabestani S, Hofmann F, Hora M, Kuczyk MA, Lam T, Marconi L, Merseburger AS, Mulders P, Powles T, Staehler M, Volpe A, Bex A. EAU guidelines on renal cell carcinoma 2014 update. Eur Urol 2015; 67: 913-924 .

[4] Escudier B, Eisen T, Stadler WM, Szczylik C, Oudard S, Siebels M, Negrier S, Chevreau C, Solska E, Desai AA, Rolland F, Demkow T, Hutson TE, Gore M, Freeman S, Schwartz B, Shan M, Simantov R, Bukowski RM; TARGET Study Group. Sorafenib in advanced clear-cell renal-cell carcinoma. N Engl J Med 2007; 356: 125-134 .

[5] Motzer RJ, Hutson TE, Tomczak P, Michaelson MD, Bukowski RM, Rixe O, Oudard S, Negrier S, Szczylik C, Kim ST, Chen I, Bycott PW, Baum CM, Figlin RA. Sunitinib versus interferon alfa in metastatic renal cell carcinoma. N Engl J Med 2007; 356: 115-124.

[6] Escudier B, Pluzanska A, Koralewski P, Ravaud A, Bracarda S, Szczylik C, Chevreau C, Filipek M, Melichar B, Bajetta E, Gorbunova V, Bay JO, Bodrogi I, Jagiello-Gruszfeld A, Moore N; AVOREN Trial investigators. Bevacizumab plus interferon alfa-2a for treatment of metastatic renal cell carcinoma: a randomised, double-blind phase III trial. Lancet 2007; 370: 2103-2111.

[7] Rixe O, Bukowski RM, Michaelson MD, Wilding G, Hudes GR, Bolte O, Motzer RJ, Bycott P, Liau KF, Freddo J, Trask PC, Kim S, Rini BI. Axitinib treatment in patients with cytokine-refractory metastatic renal-cell cancer: a phase II study. Lancet Oncol 2007; 8: 975-984.

[8] Hutson TE, Davis ID, Machiels JP, De Souza PL, Rottey S, Hong BF, Epstein RJ, Baker KL, McCann L, Crofts T, Pandite L, Figlin RA. Efficacy and safety of pazopanib in patients with metastatic renal cell carcinoma. J Clin Oncol 2010; 28: 475-480.

[9] Hudes G, Carducci M, Tomczak P, Dutcher J, Figlin R, Kapoor A, Staroslawska E, Sosman J, McDermott D, Bodrogi I, Kovacevic Z, Lesovoy V, Schmidt-Wolf IG, Barbarash O, Gokmen E, O'Toole T, Lustgarten S, Moore L, Motzer RJ; Global ARCC Trial. Temsirolimus, interferon alfa, or both for advanced renal-cell carcinoma. N Engl J Med 2007; 356: 2271-2281.

[10] Motzer RJ, Escudier B, Oudard S, Hutson TE, Porta C, Bracarda S, Grünwald V, Thompson JA, Figlin RA, Hollaender N, Urbanowitz G, Berg WJ, Kay A, Lebwohl D, Ravaud A; RECORD-1 Study Group. Efficacy of everolimus in advanced renal cell carcinoma: a double-blind, randomised, placebo-controlled phase III trial. Lancet 2008; 372: 449-456.

[11] Isono T, Chano T, Kitamura A, Yuasa T. Glucose deprivation induces G2/M transition-arrest and cell death in *N*-GlcNAc$_2$-modified protein-producing renal carcinoma cells. PLoS One 2014; 9: e96168.

[12] Isono T, Chano T, Yonese J, Yuasa T. Therapeutic inhibition of mitochondrial function induces cell death in starvation-resistant renal cell carcinomas. Sci Rep 2016; 6: e25669.

[13] Isono T. *O*-GlcNAc-specific antibody CTD110.6 cross-reacts with *N*-GlcNAc$_2$-modified proteins induced under glucose deprivation. PLoS One 2011; 6: e18959.

[14] Isono T, Chano T, Okabe H, Suzaki M. Study of global transcriptional changes of *N*-GlcNAc$_2$ proteins-producing T24 bladder carcinoma cells under glucose deprivation. PLoS One 2013; 8: e60397.

[15] Chomczynski P, Sacchi N. Single-step method of RNA isolation by acid guanidinium thiocyanate-phenol-chloroform extraction. Anal Biochem 1987; 162: 156-159.

[16] Isono T, Matsumoto T, Wada A, Suzaki M, Chano T. A global transcriptome analysis of a dog model of congestive heart failure with the human genome as a reference. J Cardiac Failure 2012; 18: 872-878.

[17] Koh MY, Nguyen V, Lemos R Jr, Darnay BG, Kiriakova G, Abdelmelek M, Ho TH, Karam J, Monzon FA, Jonasch E, Powis G. Hypoxia-induced SUMOylation of E3 ligase HAF determines specific activation of HIF2 in clear-cell renal cell carcinoma. Cancer Res 2015; 75: 316-329.

[18] Qiu B, Ackerman D, Sanchez DJ, Li B, Ochocki JD, Grazioli A, Bobrovnikova-Marjon E, Diehl JA, Keith B, Simon MC. HIF2α-Dependent Lipid Storage Promotes Endoplasmic Reticulum Homeostasis in Clear-Cell Renal Cell Carcinoma. Cancer Discov 2015; 5: 652-667.

[19] Reece KM, Richardson ED, Cook KM, Campbell TJ, Pisle ST, Holly AJ, Venzon DJ, Liewehr DJ, Chau CH, Price DK, Figg WD. Epidithiodiketopiperazines (ETPs) exhibit in vitro antiangiogenic and in vivo antitumor activity by disrupting the HIF-1α/p300 complex in a preclinical model of prostate cancer. Mol Cancer 2014; 13: 91.

[20] Krishnan B, Truong LD. Renal epithelial neoplasms: The diagnostic implications of electron microscopic study in 55 cases. Hum Pathol 2002; 33: 68-79.

[21] Kondo K, Kim WY, Lechpammer M, Kaelin WG Jr. Inhibition of HIF2alpha is sufficient to suppress pVHL-defective tumor growth. PLoS Biol 2003; 1: 439-444.

[22] Zimmer M, Doucette D, Siddiqui N, Iliopoulos O. Inhibition of hypoxia-inducible factor is sufficient for growth suppression of VHL-/- tumors. Mol Cancer Res 2004; 2: 89-95.
[23] Snell CE, Turley H, McIntyre A, Li D, Masiero M, Schofield CJ, Gatter KC, Harris AL, Pezzella F. Proline-hydroxylated hypoxia-inducible factor 1α (HIF-1α) upregulation in human tumours. PLoS One 2014; 9: e88955.